World Scientific
www.worldscientific.com

LAYER MULTIPLE SCATTERING CALCULATIONS FOR NONRECIPROCAL PHOTONIC STRUCTURES

A. CHRISTOFI* and N. STEFANOU

*Department of Solid State Physics, University of Athens,
Panepistimioupolis, GR-157 84 Athens, Greece*
aristi@ims.demokritos.gr

We present an extension of the layer-multiple-scattering method to photonic crystals of gyrotropic spheres in a homogeneous host medium. The efficiency of the method is demonstrated on specific examples of three-dimensional chiral structures and surfaces of crystals of plasma spheres in an external static uniform magnetic field that lack, simultaneously, time-reversal and space-inversion symmetries, and exhibit a nonreciprocal spectral response.

Keywords: Magnetophotonic crystals; multiple light scattering; spectral nonreciprocity.

PACS numbers: 42.70.Qs, 41.20.Jb, 42.25.Bs

1. Introduction

Nonreciprocal photonic devices play a key role in optical communication and computing technologies because of their ability to eliminate cross-talk and feedback. In this context, it has been shown that the occurrence of topologically nontrivial phenomena, such as photonic chiral edge states, in appropriately designed nonreciprocal magnetophotonic structures[1–11] allows for reflection-free one-way transport of light, which persists even in the presence of strong disorder. In general, to satisfy a sufficient condition to ensure spectral nonreciprocity, $\omega(-\mathbf{k}) \neq \omega(\mathbf{k})$, requires breaking both space-inversion and time-reversal symmetries.[12] Therefore, the development of full electrodynamic theoretical methods that can accurately describe such low-symmetry photonic structures with reduced computational effort is of primary importance.

The layer-multiple-scattering (LMS) method is a versatile and accurate full electrodynamic computational methodology for studying three-dimensional (3D) photonic crystals consisting of nonoverlapping scatterers in a homogeneous host

medium.[13,14] An important aspect of the method is that, contrary to traditional band-structure or time-domain methods, it solves Maxwell equations in frequency domain and thus one can allow the electric permittivity and magnetic permeability of any of the constituent materials to depend on the frequency, including also dissipative losses. Besides the complex photonic band structure of an infinite crystal, associated with a given crystallographic plane, the LMS method can also provide the transmission, reflection and absorption coefficients of an electromagnetic (EM) wave of any polarization incident at a given angle on a finite slab of the crystal and, therefore, it can describe an actual transmission experiment. A further advantage of the method is that it does not require periodicity in the direction perpendicular to the layers, which must only have the same two-dimensional (2D) periodicity. Therefore, a number of interesting geometries without inversion center, such as chiral structures,[15] asymmetric heterostructures,[13] stacking disorder,[16] photonic crystal slabs on homogeneous plates and substrates,[17] semi-infinite photonic crystals,[18] etc can be treated in a straightforward manner.

On the other hand, magneto-optic effects in gyrotropic materials under the action of a static uniform magnetic field break time-reversal symmetry locally, i.e., when only the propagation of light, and not the source of the magnetic field, is considered. Therefore, extension of the LMS method to gyrotropic scatterers would allow one to describe, also, nonreciprocal photonic structures. Such an extension does not involve major difficulties, since the properties of the individual scatterers enter only through the corresponding T matrix which, for gyrotropic spheres, can be obtained by applying the appropriate boundary conditions for the wave field, expanded into a spherical-wave basis, at the surface of the sphere.[19–22] In this paper we present an extension of the LMS method to photonic crystals of gyrotropic spheres and demonstrate the applicability of the method on two specific architectures of plasma spheres, without inversion center, in a static uniform magnetic field, which exhibit a nonreciprocal spectral response: A 3D chiral structure and a surface of a semi-infinite crystal.

2. Electromagnetic Waves in a Homogeneous Gyrotropic Medium

Material gyrotropy at optical and infrared frequencies is usually described by a relative permittivity tensor

$$\overset{\leftrightarrow}{\epsilon_g} = \epsilon_z \begin{pmatrix} \epsilon_r & -i\epsilon_\kappa & 0 \\ i\epsilon_\kappa & \epsilon_r & 0 \\ 0 & 0 & 1 \end{pmatrix}, \tag{1}$$

taking the gyration vector along the z-axis, and a scalar relative permeability μ_g. Starting from Maxwell equations for the spatial part of a monochromatic EM field of angular frequency ω with $\exp(-i\omega t)$ time dependence inside such a sourceless medium: $\boldsymbol{\nabla} \cdot \mathbf{B}(\mathbf{r}) = 0$, $\boldsymbol{\nabla} \cdot \mathbf{D}(\mathbf{r}) = 0$, $\boldsymbol{\nabla} \times \mathbf{E}(\mathbf{r}) = i\omega \mathbf{B}(\mathbf{r})$, $\boldsymbol{\nabla} \times \mathbf{H}(\mathbf{r}) = -i\omega \mathbf{D}(\mathbf{r})$ and the constitutive relations $\mathbf{B}(\mathbf{r}) = \mu_0 \mu_g \mathbf{H}(\mathbf{r})$ and $\mathbf{D}(\mathbf{r}) = \epsilon_0 \overset{\leftrightarrow}{\epsilon_g} \mathbf{E}(\mathbf{r})$, we obtain

the wave equation

$$\boldsymbol{\nabla} \times \boldsymbol{\nabla} \times [\epsilon_z \overset{\leftrightarrow}{\epsilon}_g^{-1} \mathbf{D}(\mathbf{r})] - q_g^2 \mathbf{D}(\mathbf{r}) = 0 \,, \tag{2}$$

with $q_g^2 = \omega^2 \epsilon_z \mu_g \epsilon_0 \mu_0 = \epsilon_z \mu_g \omega^2 / c^2$.

Following the approach of Lin and Chui,[20] we solve Eq. (2) by expanding the wavefield into the specific vector-spherical-wave basis employed in our LMS method.[13,14] For this purpose we define a set of longitudinal (irrotational) spherical wavefunctions corresponding to a wavenumber q as

$$\mathbf{F}_{Llm}(\mathbf{r}) = \frac{1}{q} \boldsymbol{\nabla}[f_l(qr) Y_{lm}(\hat{\mathbf{r}})], \quad l = 0, 1, 2, \dots; \quad m = -l, -l+1, \dots, l, \tag{3}$$

where Y_{lm} are the usual spherical harmonics and f_l may be any linear combination of the spherical Bessel function j_l and the spherical Hankel function h_l^+.[13] Similarly, we consider a set of transverse (divergenceless) spherical wavefunctions given by

$$\mathbf{F}_{Hlm}(\mathbf{r}) = f_l(qr) \mathbf{X}_{lm}(\hat{\mathbf{r}})$$

$$\mathbf{F}_{Elm}(\mathbf{r}) = \frac{i}{q} \boldsymbol{\nabla} \times [f_l(qr) \mathbf{X}_{lm}(\hat{\mathbf{r}})], \quad l = 1, 2, \dots; \quad m = -l, -l+1, \dots, l, \tag{4}$$

where $\mathbf{X}_{lm}$ are the vector spherical harmonics.[13] The above vector spherical wave functions constitute a complete basis set for the expansion of any vector field.

The divergenceless property, $\boldsymbol{\nabla} \cdot \mathbf{D} = 0$, suggests that $\mathbf{D}$ can be expanded in terms of the vector spherical wavefunctions $\mathbf{F}_{Hlm}$ and $\mathbf{F}_{Elm}$, and it does not involve $\mathbf{F}_{Llm}$. We seek such a solution in the form

$$\mathbf{D}(\mathbf{r}) = \frac{q^2}{q_g^2} \epsilon_0 \epsilon_z \sum_{l=1}^{\infty} \sum_{m=-l}^{l} [a_{Hlm} \mathbf{F}_{Hlm}(\mathbf{r}) + a_{Elm} \mathbf{F}_{Elm}(\mathbf{r})], \tag{5}$$

where a_{Hlm}, a_{Elm} are appropriate expansion coefficients that have the dimension of electric field. The choice of the prefactor $q^2 \epsilon_0 \epsilon_z / q_g^2$ is, at this stage, arbitrary. However, it is introduced here in order to obtain, as we shall see later, a simple form for the magnetic and electric multipole components of the EM field, the same as in the case of nongyrotropic materials. It can be shown (see Appendix A) that

$$\epsilon_z \overset{\leftrightarrow}{\epsilon}_g^{-1} \mathbf{D}(\mathbf{r}) = \frac{q^2}{q_g^2} \epsilon_0 \epsilon_z w_{00} \mathbf{F}_{L00}(\mathbf{r})$$

$$+ \frac{q^2}{q_g^2} \epsilon_0 \epsilon_z \sum_{l=1}^{\infty} \sum_{m=-l}^{l} [w_{lm} \mathbf{F}_{Llm}(\mathbf{r}) + \bar{d}_{lm} \mathbf{F}_{Hlm}(\mathbf{r}) + \bar{c}_{lm} \mathbf{F}_{Elm}(\mathbf{r})], \tag{6}$$

where

$$w_{00} = -\sqrt{\frac{2}{3}} \epsilon'_\kappa a_{H10} - \sqrt{\frac{2}{15}} \bar{\epsilon}'_r a_{E20} \,, \tag{7}$$

$$w_{lm} = \sum_{l'=1}^{\infty} \sum_{m'=-l'}^{l'} \left(\tilde{f}_{lm}^{l'm'} a_{Hl'm'} + \bar{f}_{lm}^{l'm'} a_{El'm'} \right), \tag{8}$$

$$\bar{d}_{lm} = \sum_{l'=1}^{\infty} \sum_{m'=-l'}^{l'} \left(\tilde{g}_{lm}^{l'm'} a_{Hl'm'} + \bar{g}_{lm}^{l'm'} a_{El'm'} \right), \tag{9}$$

$$\bar{c}_{lm} = \sum_{l'=1}^{\infty} \sum_{m'=-l'}^{l'} \left(\tilde{e}_{lm}^{l'm'} a_{Hl'm'} + \bar{e}_{lm}^{l'm'} a_{El'm'} \right), \tag{10}$$

with $\bar{\epsilon}'_r = \epsilon'_r - 1, \epsilon'_r = \epsilon_r/(\epsilon_r^2 - \epsilon_\kappa^2), \epsilon'_\kappa = -\epsilon_\kappa/(\epsilon_r^2 - \epsilon_\kappa^2)$. Explicit expressions for $\tilde{g}_{lm}^{l'm'}$, $\bar{g}_{lm}^{l'm'}$, $\tilde{e}_{lm}^{l'm'}$, $\bar{e}_{lm}^{l'm'}$, $\tilde{f}_{lm}^{l'm'}$, $\bar{f}_{lm}^{l'm'}$ are derived in Appendix A. Inserting Eqs. (5) and (6) into the wave equation (2), and taking into account Eqs. (A.1), we obtain

$$\sum_{l=1}^{\infty} \sum_{m=-l}^{l} [(q^2 \bar{d}_{lm} - q_g^2 a_{Hlm}) \mathbf{F}_{Hlm}(\mathbf{r}) + (q^2 \bar{c}_{lm} - q_g^2 a_{Elm}) \mathbf{F}_{Elm}(\mathbf{r})] = 0, \tag{11}$$

which leads to the following eigenvalue problem

$$\sum_{P'=H,E} \sum_{l'=1}^{\infty} \sum_{m'=-l'}^{l'} A_{Plm;P'l'm'} a_{P'l'm'} = \frac{q_g^2}{q^2} a_{Plm}, \tag{12}$$

where $A_{Hlm;Hl'm'} = \tilde{g}_{lm}^{l'm'}$, $A_{Hlm;El'm'} = \bar{g}_{lm}^{l'm'}$, $A_{Elm;Hl'm'} = \tilde{e}_{lm}^{l'm'}$, $A_{Elm;El'm'} = \bar{e}_{lm}^{l'm'}$. Since Eq. (2) is satisfied by $\mathbf{D}$ in the form of Eq. (5) with expansion coefficients given by any of the $j = 1, 2, \ldots$ eigenvectors $a_{Plm;j}$ of matrix $\mathbf{A}$ and vector spherical waves of wavenumber q_j obtained by the corresponding eigenvalue, the general solution for $\mathbf{D}$ can be written in the form

$$\mathbf{D}(\mathbf{r}) = \sum_j b_j \frac{q_j^2}{q_g^2} \epsilon_0 \epsilon_z \sum_{l=1}^{\infty} \sum_{m=-l}^{l} \left[a_{Hlm;j} \mathbf{F}_{Hlm}(\mathbf{r}) + a_{Elm;j} \mathbf{F}_{Elm}(\mathbf{r}) \right], \tag{13}$$

where the expansion coefficients b_j are to be determined, in general, by the boundary conditions. With $\mathbf{D}$ given by Eq. (13), it follows from $\mathbf{H}(\mathbf{r}) = (-i/\omega\mu_0\mu_g)\nabla \times \mathbf{E}(\mathbf{r})$ and from the constitutive relations that the $\mathbf{E}$ and $\mathbf{H}$ fields take the form

$$\mathbf{E}(\mathbf{r}) = \sum_j b_j \left\{ \frac{q_j^2}{q_g^2} w_{00;j} \mathbf{F}_{L00}(\mathbf{r}) \right.$$

$$\left. + \sum_{l=1}^{\infty} \sum_{m=-l}^{l} \left[\frac{q_j^2}{q_g^2} w_{lm;j} \mathbf{F}_{Llm}(\mathbf{r}) + a_{Hlm;j} \mathbf{F}_{Hlm}(\mathbf{r}) + a_{Elm;j} \mathbf{F}_{Elm}(\mathbf{r}) \right] \right\} \tag{14}$$

and

$$\mathbf{H}(\mathbf{r}) = \sum_j b_j \frac{q_j}{\omega\mu_0\mu_g} \sum_{l=1}^{\infty} \sum_{m=-l}^{l} \left[a_{Elm;j} \mathbf{F}_{Hlm}(\mathbf{r}) - a_{Hlm;j} \mathbf{F}_{Elm}(\mathbf{r}) \right], \tag{15}$$

respectively, where $w_{lm;j} = \sum_{l'=1}^{\infty} \sum_{m'=-l'}^{l'} (\tilde{f}_{lm}^{l'm'} a_{Hl'm';j} + \bar{f}_{lm}^{l'm'} a_{El'm';j})$ and $w_{00;j} = -\sqrt{(2/3)}\epsilon'_\kappa a_{H10;j} - \sqrt{(2/15)}\bar{\epsilon}'_r a_{E20;j}$.

3. Scattering by a Gyrotropic Sphere

We assume a homogeneous gyrotropic sphere of radius S, characterized by EM parameters $\overset{\leftrightarrow}{\epsilon}_g$ and μ_g, centered at the origin of coordinates in a host medium characterized by ϵ_h and μ_h. The sphere is illuminated by a plane EM wave. Using the methodology presented in Sec. 2, we write the corresponding EM field inside the sphere as

$$
\mathbf{E}_{\mathrm{in}}(\mathbf{r}) = \sum_j b_j \Bigg\{ \frac{q_j^2}{q_g^2} w_{00;j} \frac{1}{q_j} \boldsymbol{\nabla}[j_0(q_j r) Y_0^0(\hat{\mathbf{r}})]
$$

$$
+ \sum_{l=1}^{\infty} \sum_{m=-l}^{l} \left[\frac{q_j^2}{q_g^2} w_{lm;j} \frac{1}{q_j} \boldsymbol{\nabla}[j_l(q_j r) Y_l^m(\hat{\mathbf{r}})] + a_{Hlm;j} j_l(q_j r) \mathbf{X}_{lm}(\hat{\mathbf{r}}) \right.
$$

$$
\left. + a_{Elm;j} \frac{i}{q_j} \boldsymbol{\nabla} \times j_l(q_j r) \mathbf{X}_{lm}(\hat{\mathbf{r}}) \right] \Bigg\}. \tag{16}
$$

$$
\mathbf{H}_{\mathrm{in}}(\mathbf{r}) = \sum_j b_j \frac{q_j}{\omega \mu_0 \mu_g} \sum_{l=1}^{\infty} \sum_{m=-l}^{l} \left[a_{Elm;j} j_l(q_j r) \mathbf{X}_{lm}(\hat{\mathbf{r}}) \right.
$$

$$
\left. - a_{Hlm;j} \frac{i}{q_j} \boldsymbol{\nabla} \times j_l(q_j r) \mathbf{X}_{lm}(\hat{\mathbf{r}}) \right]. \tag{17}
$$

Outside the sphere we express the EM field, as usual,[13,14] as a combination of the incident and scattered fields

$$
\mathbf{E}_{out}(\mathbf{r}) = \sum_{l=1}^{\infty} \sum_{m=-l}^{l} \left[a_{Hlm}^0 j_l(q_h r) \mathbf{X}_{lm}(\hat{\mathbf{r}}) + \frac{i}{q_h} a_{Elm}^0 \boldsymbol{\nabla} \times j_l(q_h r) \mathbf{X}_{lm}(\hat{\mathbf{r}}) \right.
$$

$$
\left. + a_{Hlm}^+ h_l^+(q_h r) \mathbf{X}_{lm}(\hat{\mathbf{r}}) + \frac{i}{q_h} a_{Elm}^+ \boldsymbol{\nabla} \times h_l^+(q_h r) \mathbf{X}_{lm}(\hat{\mathbf{r}}) \right], \tag{18}
$$

$$
\mathbf{H}_{out}(\mathbf{r}) = \sqrt{\frac{\epsilon_h \epsilon_0}{\mu_h \mu_0}} \sum_{l=1}^{\infty} \sum_{m=-l}^{l} \left[a_{Elm}^0 j_l(q_h r) \mathbf{X}_{lm}(\hat{\mathbf{r}}) - \frac{i}{q_h} a_{Hlm}^0 \boldsymbol{\nabla} \times j_l(q_h r) \mathbf{X}_{lm}(\hat{\mathbf{r}}) \right.
$$

$$
\left. + a_{Elm}^+ h_l^+(q_h r) \mathbf{X}_{lm}(\hat{\mathbf{r}}) - \frac{i}{q_h} a_{Hlm}^+ \boldsymbol{\nabla} \times h_l^+(q_h r) \mathbf{X}_{lm}(\hat{\mathbf{r}}) \right], \tag{19}
$$

where $q_h = \omega\sqrt{\epsilon_h \mu_h}/c$ and the coefficients a_{Plm}^0, a_{Plm}^+ refer to the incident and scattered waves, respectively. Applying the boundary conditions of continuity of the tangential components of the EM field at the surface of the sphere we obtain

$$
a_{Hlm}^0 = -\frac{h_l^+(q_h S)}{j_l(q_h S)} a_{Hlm}^+ + \sum_j \frac{j_l(q_j S)}{j_l(q_h S)} a_{Hlm;j} b_j \tag{20}
$$

$$
a_{Elm}^0 = -\frac{h_l^+(q_h S)}{j_l(q_h S)} a_{Elm}^+ + \sum_j \frac{\mu_h q_j j_l(q_j S)}{\mu_g q_h j_l(q_h S)} a_{Elm;j} b_j, \tag{21}
$$

$$a_{Hlm}^0 = -\frac{[xh_l^+(x)]'_{q_hS}}{[xj_l(x)]'_{q_hS}}a_{Hlm}^+ + \sum_j \frac{\mu_h[xj_l(x)]'_{q_jS}}{\mu_g[xj_l(x)]'_{q_hS}}a_{Hlm;j}b_j \,, \tag{22}$$

$$a_{Elm}^0 = -\frac{[xh_l^+(x)]'_{q_hS}}{[xj_l(x)]'_{q_hS}}a_{Elm}^+ + \sum_j \frac{q_h[xj_l(x)]'_{q_jS}}{q_j[xj_l(x)]'_{q_hS}}a_{Elm;j}b_j$$

$$- \sum_j \frac{\sqrt{l(l+1)}q_j q_h j_l(q_jS)}{q_g^2[xj_l(x)]'_{q_hS}}w_{lm;j}b_j \,. \tag{23}$$

Equations (20)–(23) can be rewritten in matrix form

$$\mathbf{a}^0 = \mathbf{\Lambda}\mathbf{a}^+ + \mathbf{U}\mathbf{b} \,, \tag{24}$$

$$\mathbf{a}^0 = \mathbf{\Lambda'}\mathbf{a}^+ + \mathbf{V}\mathbf{b} \,, \tag{25}$$

where

$$\Lambda_{Plm;P'l'm'} = -\frac{h_l^+(q_hS)}{j_l(q_hS)}\delta_{PP'}\delta_{ll'}\delta_{mm'} \,,$$

$$\Lambda'_{Plm;P'l'm'} = -\frac{[xh_l^+(x)]'_{q_hS}}{[xj_l(x)]'_{q_hS}}\delta_{PP'}\delta_{ll'}\delta_{mm'} \,, \tag{26}$$

$$U_{Hlm;j} = \frac{j_l(q_jS)}{j_l(q_hS)}a_{Hlm;j} \,, \quad U_{Elm;j} = \frac{\mu_h q_j j_l(q_jS)}{\mu_g q_h j_l(q_hS)}a_{Elm;j} \,, \tag{27}$$

$$V_{Hlm;j} = \frac{\mu_h[xj_l(x)]'_{q_jS}}{\mu_g[xj_l(x)]'_{q_hS}}a_{Hlm;j} \,,$$

$$V_{Elm;j} = \frac{q_h[xj_l(x)]'_{q_jS}}{q_j[xj_l(x)]'_{q_hS}}a_{Elm;j} - \frac{\sqrt{l(l+1)}q_j q_h j_l(q_jS)}{q_g^2[xj_l(x)]'_{q_hS}}w_{lm;j} \,. \tag{28}$$

Equations (24) and (25) can be solved to give

$$\mathbf{b} = \mathbf{R}\mathbf{a}^0 \tag{29}$$

$$\mathbf{a}^+ = \mathbf{T}\mathbf{a}^0 \,, \tag{30}$$

where $\mathbf{R} = (\mathbf{U} + \mathbf{\Lambda}\mathbf{Z})^{-1}$, $\mathbf{Z} = (\mathbf{\Lambda} - \mathbf{\Lambda'})^{-1}(\mathbf{V} - \mathbf{U})$, $\mathbf{T} = \mathbf{Z}\mathbf{R}$.

Equation (30) defines the so-called scattering T matrix, which relates the expansion coefficients (in the given spherical-wave basis) of the scattered field to those of the incident field. For a sphere described by a relative permittivity tensor in the form of Eq. (1), the T matrix has a block diagonal form: $T_{Plm;P'l'm'} = T_{Pl;P'l'}^{(m)}\delta_{mm'}$. Moreover, $T_{Pl;P'l'}^{(m)}$ vanishes identically if the magnetic (H)/electric (E) multipoles corresponding to Pl and $P'l'$ do not have the same parity, even or odd, which means that the T matrix in a given m subspace is further reduced into two submatrices. These symmetry properties, however, do not hold in any coordinate system. If α, β, γ are the Euler angles transforming an arbitrarily chosen coordinate system into

the given coordinate system in which the relative permittivity tensor has the form of Eq. (1), the T matrix is given by

$$T_{Plm;P'l'm'} = \sum_{m''} D_{mm''}^{(l)}(\alpha, \beta, \gamma) T_{Pl;P'l'}^{(m'')} D_{m''m'}^{(l')}(-\gamma, -\beta, -\alpha) \,, \tag{31}$$

where $D^{(l)}$ are the appropriate transformation matrices associated with the l irreducible representation of the $O(3)$ group.[23]

4. The Layer-Multiple-Scattering Method

In the spirit of the multiple-scattering approach, the scattering properties of a composite structure are obtained from those of its constituent building units. Once the T matrix of the gyrotropic spheres is calculated, in-plane multiple scattering for a 2D periodic array of such spheres is described in the given spherical-wave basis using the calculated T matrix and appropriate propagator functions.[13,14] For multilayer structures with the same 2D periodicity, the LMS method describes interlayer coupling by properly combining the transmission and reflection matrices of the component layers, so as to describe multiple scattering between the layers to any order, in a plane-wave representation defined as follows. The component of the wavevector of the incident plane wave parallel to the layers, $\mathbf{q}_\parallel$, is written as $\mathbf{q}_\parallel = \mathbf{k}_\parallel + \mathbf{g}'$, where $\mathbf{k}_\parallel$, the reduced wavevector in the surface Brillouin zone, is a conserved quantity in the scattering process and $\mathbf{g}'$ is a certain reciprocal vector of the given 2D lattice. Therefore, the wavevector of the incident wave has the form $\mathbf{K}_{\mathbf{g}'}^\pm = \mathbf{k}_\parallel + \mathbf{g}' \pm [q_h^2 - (\mathbf{k}_\parallel + \mathbf{g}')^2]^{1/2}\hat{\mathbf{e}}_z$, where q_h is the wavenumber, $\hat{\mathbf{e}}_z$ is the unit vector along the z-axis and the $+$ or $-$ sign refers to incidence from $z < 0$ or from $z > 0$, i.e., a wave propagating towards the positive or negative z-direction, respectively. Since $\mathbf{k}_\parallel$ and the angular frequency ω are conserved quantities in the elastic scattering process, the scattered field consists of a series of plane waves with wavevectors $\mathbf{K}_{\mathbf{g}}^\pm = \mathbf{k}_\parallel + \mathbf{g} \pm [q_h^2 - (\mathbf{k}_\parallel + \mathbf{g})^2]^{1/2}\hat{\mathbf{e}}_z$, $\forall \mathbf{g}$ and polarizations along $\hat{\mathbf{e}}_1$ and $\hat{\mathbf{e}}_2$ (polar and azimuthal unit vectors, respectively, associated with every $\mathbf{K}_{\mathbf{g}}^\pm$). Corresponding circularly polarized plane waves are defined by the unit vectors $\hat{\mathbf{e}}_L = (\hat{\mathbf{e}}_1 + i\hat{\mathbf{e}}_2)/\sqrt{2}$ and $\hat{\mathbf{e}}_R = (\hat{\mathbf{e}}_1 - i\hat{\mathbf{e}}_2)/\sqrt{2}$, for left circular polarization (LCP) and right circular polarization (RCP), respectively. It is worth noting that, though the scattered field consists, in general, of a number of diffracted beams corresponding to different 2D reciprocal lattice vectors $\mathbf{g}$, only beams for which $\mathbf{K}_{\mathbf{g}z}^\pm$ is real constitute propagating waves. When $(\mathbf{k}_\parallel + \mathbf{g})^2 > q_h^2$ we have an evanescent beam and the corresponding unit vectors $\hat{\mathbf{e}}_1$, $\hat{\mathbf{e}}_2$ become complex but they are still orthonormal: $\hat{\mathbf{e}}_p \cdot \hat{\mathbf{e}}_{p'} = \delta_{pp'}$, $p(p') = 1, 2$.

The ratio of the transmitted or reflected energy flux to the energy flux associated with the incident wave defines the transmittance or reflectance, respectively, of a multilayer slab. On the other hand, for a 3D crystal consisting of an infinite periodic sequence of layers, stacked along the z-direction, applying the Bloch condition for the wave field in the region between two consecutive unit slabs leads to

an eigenvalue equation, which gives the z component of the Bloch wave vector, k_z, for the given ω and $\mathbf{k}_\parallel$. The eigenvalues $k_z(\omega, \mathbf{k}_\parallel)$, looked upon as functions of real ω, define, for each $\mathbf{k}_\parallel$, lines in the complex k_z plane. Taken together they constitute the complex band structure of the infinite crystal associated with the given crystallographic plane. A line of given $\mathbf{k}_\parallel$ may be real (in the sense that k_z is real) over certain frequency regions, and be complex (in the sense that k_z is complex) for ω outside these regions. It turns out that, for given $\mathbf{k}_\parallel$ and ω, out of the eigenvalues $k_z(\omega, \mathbf{k}_\parallel)$ none or, at best, a few are real and the corresponding eigenvectors represent propagating modes of the EM field in the given infinite crystal. The remaining eigenvalues $k_z(\omega, \mathbf{k}_\parallel)$ are complex and the corresponding eigenvectors represent evanescent waves. These have an amplitude which increases exponentially in the positive or negative z-direction and, unlike the propagating waves, do not exist as physical entities in the infinite crystal. However, they are an essential part of the physical solutions of the EM field in a slab of finite thickness. A region of frequency where propagating waves do not exist, for given $\mathbf{k}_\parallel$, constitutes a frequency gap of the EM field for the given $\mathbf{k}_\parallel$. If over a frequency region no propagating wave exists whatever the value of $\mathbf{k}_\parallel$, then this region constitutes an absolute frequency gap.

5. Applications

We shall now apply our generalized LMS method to describe the optical response of some structures of plasma spheres, without space inversion symmetry, under the action of an external static uniform magnetic field. In all of the cases we studied we obtained good convergence by truncating the spherical-wave expansion at $l_{\max} = 6$ and taking into account 45 2D reciprocal lattice vectors.

The response of a plasma to an external EM field can be described by a relative magnetic permeability $\mu_p = 1$ and by the simple yet effective Drude relative electric permittivity[24]

$$\epsilon_p = 1 - \frac{\omega_p^2}{\omega(\omega + i/\tau)}, \tag{32}$$

where τ is the relaxation time of the free carriers and ω_p is the bulk plasma frequency: $\omega_p^2 = ne^2/(m\epsilon_0)$, with n, $-e$ and m the carrier density, charge and mass, respectively, which naturally introduces c/ω_p as the length unit. We note that, assuming $\hbar\omega_p \simeq 10$ eV, which is a typical value for metals, c/ω_p corresponds to about 20 nm. For semiconductors, on the other hand, as their carrier densities can be easily varied within a broad range of values, which are much lower than those in metals, the plasma frequency is much smaller (typically at mid- and far-infrared frequencies) and the length unit c/ω_p increases accordingly.

In the presence of a static uniform magnetic field, $\mathbf{B}$, the response of a plasma to a time-harmonic EM wave of angular frequency ω, with electric-field component $\mathbf{E} = \mathbf{E}_0 \exp(-i\omega t)$, is described by the equation of motion of the electrons: $m\ddot{\mathbf{r}} = -m\tau^{-1}\dot{\mathbf{r}} - e\mathbf{E} - e\dot{\mathbf{r}} \times \mathbf{B}$. The resulting polarization density, $\mathbf{P} = -ne\mathbf{r}$, defines an

electric displacement vector $\mathbf{D} = \epsilon_0 \mathbf{E} + \mathbf{P}$ and finally yields the relative electric permittivity tensor $\overset{\leftrightarrow}{\epsilon}_g$ of the magnetized plasma through $\mathbf{D} = \epsilon_0 \overset{\leftrightarrow}{\epsilon}_g \mathbf{E}$. Defining the cyclotron resonance frequency, $\omega_c = eB/m$, if $\mathbf{B}$ is oriented along the z-direction, after some straightforward algebra we find that $\overset{\leftrightarrow}{\epsilon}_g$ has the gyrotropic form

$$\overset{\leftrightarrow}{\epsilon}_g = \begin{pmatrix} 1 - \dfrac{\omega_p^2[1 + i/(\tau\omega)]}{(\omega + i/\tau)^2 - \omega_c^2} & i\dfrac{\omega_c}{\omega}\dfrac{\omega_p^2}{(\omega + i/\tau)^2 - \omega_c^2} & 0 \\ -i\dfrac{\omega_c}{\omega}\dfrac{\omega_p^2}{(\omega + i/\tau)^2 - \omega_c^2} & 1 - \dfrac{\omega_p^2[1 + i/(\tau\omega)]}{(\omega + i/\tau)^2 - \omega_c^2} & 0 \\ 0 & 0 & 1 - \dfrac{\omega_p^2}{\omega(\omega + i/\tau)} \end{pmatrix}. \quad (33)$$

We note that, by setting $\omega_c = 0$, $\overset{\leftrightarrow}{\epsilon}_g$ becomes a diagonal tensor with all of its diagonal elements equal to ϵ_p given by Eq. (32), as expected. In our calculations we shall neglect dissipative losses ($\tau^{-1} = 0$) in order to ensure an unambiguous interpretation of the photonic band structure.

We first consider a tetragonal crystal defined by the primitive lattice vectors $\mathbf{a}_1 = (a, 0, 0)$, $\mathbf{a}_2 = (0, a, 0)$, $\mathbf{a}_3 = (0, 0, d)$ and a basis of four plasma spheres, of radius S, centered at $(0, 0, 0)$, $(b, 0, d/4)$, $(b, b, d/2)$, $(0, b, 3d/4)$, as shown in Fig. 1, embedded in a homogeneous host medium of relative electric permittivity $\epsilon_h = 1$ and magnetic permeability $\mu_h = 1$. For the crystal under consideration, we take $a = c/\omega_p$, $d = 2c/\omega_p$, $S = 0.2c/\omega_p$ and $b = 0.3c/\omega_p$. The photonic band structure of this crystal is characterized by the presence of narrow bands, which originate
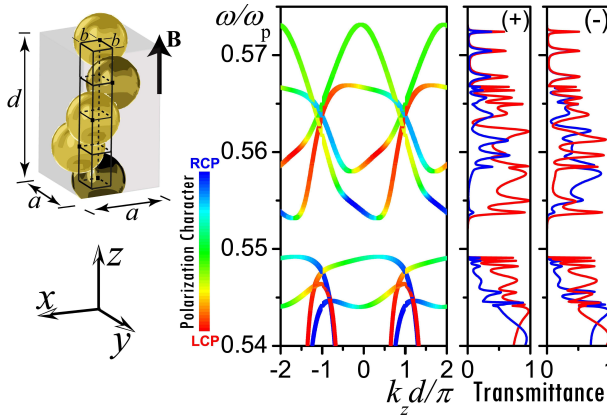

Fig. 1. Left-hand panel: The unit cell of a chiral crystal described by a tetragonal lattice, of lattice constants a and d, with a basis of four Drude spheres of radius $S = 0.2c/\omega_p$, in a helical arrangement along the z-direction ($a = c/\omega_p, d = 2c/\omega_p, b = 0.3c/\omega_p$). Right-hand panel: The photonic band structure of this crystal under the action of a static uniform magnetic field corresponding to $\omega_c = 0.01\omega_p$ along the [001] direction, in the frequency region about the lowest flat bands. Next to the band diagram we depict the corresponding transmittance of a (001) slab of the crystal, consisting of 16 layers of spheres, for LCP and RCP light incident in (+) and opposite to (−) the direction of the static magnetic field.

from the dipole particle-plasmon modes of the individual spheres, at $\omega_1 = 0.575\omega_p$, weakly interacting between them. These flat bands hybridize with the extended bands that would be in an underlying homogeneous effective medium, giving rise to frequency gaps and negative-slope dispersion,[25] while a Dirac point was identified at the center of the first Brillouin zone.[26] It is worth noting that, though this crystal does not possess space-inversion symmetry, the symmetry $\omega(-\mathbf{k}) = \omega(\mathbf{k})$ persists because of time-reversal symmetry.

If we assume that a static uniform magnetic field is applied along the z-direction, the scalar Drude permittivity of the plasma spheres becomes a tensor, $\overset{\leftrightarrow}{\epsilon}_g$, given by Eq. (33) with $\tau^{-1} = 0$ since we neglect dissipative losses. In Fig. 1 we depict the calculated photonic band structure in this case, in the frequency region of the lowest flat bands assuming $\omega_c = 0.01\omega_p$. This value of ω_c, though it is by an order of magnitude smaller than that used by Yu *et al.*,[27] for metals corresponds to a prohibitively strong magnetic field, of the order of 10^3 T, but for semiconductors the field becomes much weaker, of the order of 1 T or less. As dictated by group theory, the bands along this direction are nondegenerate and the associated Bloch modes are characterized by a different degree of LCP and RCP admixture that varies along a specific band. However, now, because of the lower symmetry due to the static magnetic field, all degeneracies at the high symmetry points are also removed. For example, as shown in Fig. 1, the bands do not cross each other at the Dirac point at the center of the first Brillouin zone and split apart, as anticipated by Yannopapas on the basis of a simple model.[26] However, here, in addition to this splitting, spectral nonreciprocity, $\omega(-\mathbf{k}) \neq \omega(\mathbf{k})$, is also clearly manifested as a result of time-reversal-symmetry breaking in conjunction with the lack of space-inversion symmetry. We note that the invariance of Bloch modes that differ by a reciprocal lattice vector, i.e., here by $(0, 0, 2\pi n/d)$, $n = 0, \pm 1, \pm 2, \ldots$, is not violated.

In Fig. 1, next to the band diagram, we depict the corresponding transmittance of a (001) slab of the crystal consisting of 16 layers of spheres, for LCP and RCP light incident in (+) and opposite to (−) the direction of the static magnetic field. Though there is no frequency region where only modes with positive or negative group velocity exist, interestingly, in the range from $0.554\omega_p$ to $0.558\omega_p$ we have polarization-selective one-way transmission, where LCP waves are predominantly transmitted in the direction of the static magnetic field while RCP waves are transmitted only in the opposite direction.

We next consider a semi-infinite fcc crystal of plasma spheres, grown along its [001] direction, as shown in the left-hand panel of Fig. 2. The spheres have a radius $S = c/\omega_p$ and the nearest neighbor distance in the fcc lattice is $a_0 = 2.2c/\omega_p$. It has been recently shown that this crystal supports surface, so-called Tamm, states at its (001) surface.[18] The dispersion curve, $\omega(\mathbf{k}_\parallel)$, of an optical Tamm state lies outside the light cone in the host medium and at the same time within a frequency gap of the crystal. This ensures that the associated EM field decreases exponentially on either side of the surface. Moreover, the dispersion of a surface state satisfies the
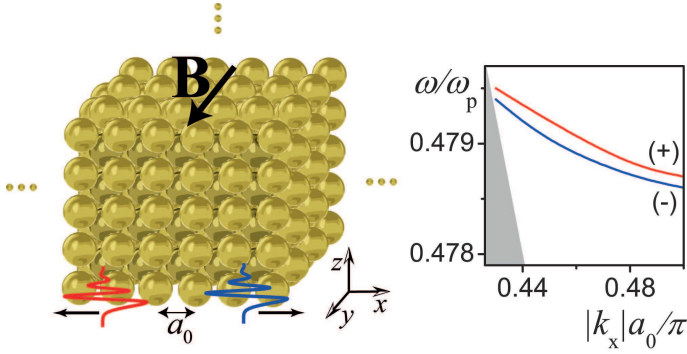
Fig. 2. Left-hand panel: A semi-infinite fcc crystal of Drude spheres (nearest neighbor distance: $a_0 = 2.2c/\omega_p$; sphere radius: $S = c/\omega_p$), grown along its [001] direction, with surface states (schematic representation). Right-hand panel: The dispersion diagram of an actual surface state at the (001) surface of this crystal under the action of a static uniform magnetic field corresponding to $\omega_c = 0.01\omega_p$ along the [110] crystallographic direction which is taken to be the y-axis. The $(+)$ and $(-)$ signs denote positive and negative values of k_x, which correspond to backward and forward propagating modes, respectively. The shaded area marks the region of the frequency bands.

reciprocity condition $\omega(-\mathbf{k}_\parallel) = \omega(\mathbf{k}_\parallel)$. However, if an external static uniform magnetic field is applied parallel to the surface, say along the y-direction, the dispersion of the surface state changes and becomes nonreciprocal: $\omega(-k_x) \neq \omega(k_x)$. This is shown in Fig. 2, which displays the dispersion of an optical Tamm state at the (001) surface of the crystal of plasma spheres under consideration, in the positive $(+)$ and negative $(-)$ x-direction. Reversal of the magnetic field direction has the same effect as reversal of the propagation direction $(k_x \to -k_x)$ while, if the magnetic field is perpendicular to the surface or parallel to the propagation direction, nonreciprocity is not encountered. Since in the present case the static magnetic field is not oriented along the z-direction, which is by definition the direction of growth of the crystal in the LMS method, the calculations involved require transforming the T matrix according to Eq. (31) using the appropriate Euler angles: $\alpha = 90°$, $\beta = 90°$, $\gamma = 0°$.[28]

As a result of the spectral splitting of the dispersion curves associated with the forward and backward propagating waves, within a short frequency range near their band edges, only modes propagating in one direction exist, as shown in Fig. 2. The relative spectral shift of the bands depends on the magnitude of the external field, which allows for the design of tunable surface states for one-way light transport. A similar nonreciprocal behavior has been reported for surface modes at truncated one-dimensional magnetophotonic crystals.[29]

6. Conclusion

In summary, we extended the full-electrodynamic LMS method to photonic structures of gyrotropic spheres with arbitrarily oriented gyration vector. The

applicability and efficiency of the method is demonstrated by two illustrative examples of bulk and surface geometries without inversion center, namely a 3D chiral structure and a semi-infinite fcc crystal of magnetized plasma nanospheres. Spectral nonreciprocity of bulk and surface states, which emerges as a result of the simultaneous lack of space-inversion and time-reversal symmetries, is demonstrated in the Faraday and Voigt configurations, respectively.

Acknowledgments

Appendix A. Derivation of Explicit Expressions for the $\tilde{g}_{lm}^{l'm'}$, $\bar{g}_{lm}^{l'm'}$, $\tilde{e}_{lm}^{l'm'}$, $\bar{e}_{lm}^{l'm'}$, $\tilde{f}_{lm}^{l'm'}$, $\bar{f}_{lm}^{l'm'}$ Coefficients

In this Appendix we derive explicit expressions for the expansion coefficients $\tilde{g}_{lm}^{l'm'}$, $\bar{g}_{lm}^{l'm'}$, $\tilde{e}_{lm}^{l'm'}$, $\bar{e}_{lm}^{l'm'}$, $\tilde{f}_{lm}^{l'm'}$, $\bar{f}_{lm}^{l'm'}$, which are slightly different from those of Lin and Chui[20] because of the different definition of the vector spherical waves. The vector spherical wavefunctions satisfy the following equations

$$\boldsymbol{\nabla} \times \mathbf{F}_{Llm} = 0 \,,$$
$$\boldsymbol{\nabla} \times \mathbf{F}_{Hlm} = -iq\mathbf{F}_{Elm} \,,$$
$$\boldsymbol{\nabla} \times \mathbf{F}_{Elm} = iq\mathbf{F}_{Hlm} \,, \tag{A.1}$$
$$\boldsymbol{\nabla} \times \boldsymbol{\nabla} \times \mathbf{F}_{Hlm} - q^2\mathbf{F}_{Hlm} = 0 \,,$$
$$\boldsymbol{\nabla} \times \boldsymbol{\nabla} \times \mathbf{F}_{Elm} - q^2\mathbf{F}_{Elm} = 0 \,.$$

Moreover, they are orthogonal in the sense that

$$\int_0^{2\pi}\int_0^\pi \bar{\mathbf{F}}_{Hlm} \cdot \mathbf{F}_{El'm'} \sin\theta d\theta d\phi = 0 \,,$$

$$\int_0^{2\pi}\int_0^\pi \bar{\mathbf{F}}_{Llm} \cdot \mathbf{F}_{Hl'm'} \sin\theta d\theta d\phi = 0 \,,$$

$$\int_0^{2\pi}\int_0^\pi \bar{\mathbf{F}}_{Hlm} \cdot \mathbf{F}_{Hl'm'} \sin\theta d\theta d\phi = f_l^2 \delta_{ll'}\delta_{mm'}$$

$$\int_0^{2\pi}\int_0^\pi \bar{\mathbf{F}}_{Elm} \cdot \mathbf{F}_{El'm'} \sin\theta d\theta d\phi = \frac{1}{2l+1}[(l+1)f_{l-1}^2 + lf_{l+1}^2]\delta_{ll'}\delta_{mm'} \,, \tag{A.2}$$

$$\int_0^{2\pi}\int_0^\pi \bar{\mathbf{F}}_{Llm} \cdot \mathbf{F}_{Ll'm'} \sin\theta d\theta d\phi = \frac{1}{2l+1}[lf_{l-1}^2 + (l+1)f_{l+1}^2]\delta_{ll'}\delta_{mm'} \,,$$

$$\int_0^{2\pi}\int_0^\pi \bar{\mathbf{F}}_{Llm} \cdot \mathbf{F}_{El'm'} \sin\theta d\theta d\phi = \frac{\psi_l}{2l+1}[f_{l+1}^2 - f_{l-1}^2]\delta_{ll'}\delta_{mm'} \,,$$

where $\psi_l = \sqrt{l(l+1)}$ and the bar symbol over a vector spherical wavefunction denotes complex conjugation only on its angular part.

It can be readily shown that

$$
\epsilon_z \overset{\leftrightarrow}{\epsilon_g}{}^{-1} = \begin{pmatrix} \epsilon_r' & -i\epsilon_\kappa' & 0 \\ i\epsilon_\kappa' & \epsilon_r' & 0 \\ 0 & 0 & 1 \end{pmatrix}, \tag{A.3}
$$

which in dyadic form can be rewritten as

$$
\epsilon_z \overset{\leftrightarrow}{\epsilon_g}{}^{-1} = (\epsilon_r' - \epsilon_\kappa')\hat{\mathbf{e}}_-\hat{\mathbf{e}}_+ + (\epsilon_r' + \epsilon_\kappa')\hat{\mathbf{e}}_+\hat{\mathbf{e}}_- + \hat{\mathbf{e}}_0\hat{\mathbf{e}}_0 , \tag{A.4}
$$

where $\epsilon_r' = \epsilon_r/(\epsilon_r^2 - \epsilon_\kappa^2)$ and $\epsilon_\kappa' = -\epsilon_\kappa/(\epsilon_r^2 - \epsilon_\kappa^2)$ and $\hat{\mathbf{e}}_+ = (\hat{\mathbf{e}}_x + i\hat{\mathbf{e}}_y)/\sqrt{2}$, $\hat{\mathbf{e}}_0 = \hat{\mathbf{e}}_z$, $\hat{\mathbf{e}}_- = (\hat{\mathbf{e}}_x - i\hat{\mathbf{e}}_y)/\sqrt{2}$. Rewritten in terms of $\hat{\mathbf{e}}_\pm$ and $\hat{\mathbf{e}}_0$ the vector spherical wavefunctions take the form

$$
\mathbf{F}_{Hlm} = \frac{f_l}{\psi_l}\left(\sqrt{2}\alpha_l^{-m}Y_{lm-1}\hat{\mathbf{e}}_+ + \sqrt{2}\alpha_l^m Y_{lm+1}\hat{\mathbf{e}}_- + mY_{lm}\hat{\mathbf{e}}_0\right), \tag{A.5}
$$

$$
\begin{aligned}
\mathbf{F}_{Elm} = &\left[\frac{-l}{\sqrt{2}\psi_l}\sqrt{\frac{(l-m+2)(l-m+1)}{(2l+1)(2l+3)}}Y_{l+1m-1}f_{l+1}\right.\\
&\left.+\frac{l+1}{\sqrt{2}\psi_l}\sqrt{\frac{(l+m)(l+m-1)}{(2l-1)(2l+1)}}Y_{l-1m-1}f_{l-1}\right]\hat{\mathbf{e}}_+\\
&+\left[\frac{l}{\sqrt{2}\psi_l}\sqrt{\frac{(l+m+2)(l+m+1)}{(2l+1)(2l+3)}}Y_{l+1m+1}f_{l+1}\right.\\
&\left.+\frac{-(l+1)}{\sqrt{2}\psi_l}\sqrt{\frac{(l-m)(l-m-1)}{(2l-1)(2l+1)}}Y_{l-1m+1}f_{l-1}\right]\hat{\mathbf{e}}_-\\
&+\left[\frac{-l}{\psi_l}\sqrt{\frac{(l+m+1)(l-m+1)}{(2l+1)(2l+3)}}Y_{l+1m}f_{l+1}\right.\\
&\left.+\frac{-(l+1)}{\psi_l}\sqrt{\frac{(l+m)(l-m)}{(2l-1)(2l+1)}}Y_{l-1m}f_{l-1}\right]\hat{\mathbf{e}}_0 , \tag{A.6}
\end{aligned}
$$

$$
\begin{aligned}
\mathbf{F}_{Llm} = &\left[\frac{-1}{\sqrt{2}}\sqrt{\frac{(l-m+2)(l-m+1)}{(2l+1)(2l+3)}}Y_{l+1m-1}f_{l+1}\right.\\
&\left.-\frac{1}{\sqrt{2}}\sqrt{\frac{(l+m)(l+m-1)}{(2l-1)(2l+1)}}Y_{l-1m-1}f_{l-1}\right]\hat{\mathbf{e}}_+\\
&+\left[\frac{1}{\sqrt{2}}\sqrt{\frac{(l+m+2)(l+m+1)}{(2l+1)(2l+3)}}Y_{l+1m+1}f_{l+1}\right.\\
&\left.+\frac{1}{\sqrt{2}}\sqrt{\frac{(l-m)(l-m-1)}{(2l-1)(2l+1)}}Y_{l-1m+1}f_{l-1}\right]\hat{\mathbf{e}}_-
\end{aligned}
$$

$$- \left[\sqrt{\frac{(l+m+1)(l-m+1)}{(2l+1)(2l+3)}} Y_{l+1 m} f_{l+1} \right.$$

$$\left. + \sqrt{\frac{(l+m)(l-m)}{(2l-1)(2l+1)}} Y_{l-1 m} f_{l-1} \right] \hat{\mathbf{e}}_0 , \tag{A.7}$$

where $\alpha_l^m = (1/2)[(l-m)(l+m+1)]^{1/2}$. Multiplying Eq. (A.5) by the dyad $\epsilon_z \overset{\leftrightarrow}{\epsilon_g}^{-1}$ gives

$$\epsilon_z \overset{\leftrightarrow}{\epsilon_g}^{-1} \mathbf{F}_{Hlm} = \frac{f_l}{\psi_l} \left[\sqrt{2} \alpha_l^{-m} Y_{lm-1}(\epsilon_r' + \epsilon_\kappa') \hat{\mathbf{e}}_+ \right.$$

$$\left. + \sqrt{2} \alpha_l^m Y_{lm+1}(\epsilon_r' - \epsilon_\kappa') \hat{\mathbf{e}}_- + m Y_{lm} \hat{\mathbf{e}}_0 \right]$$

$$= \sum_{qp} (\tilde{g}_{qp}^{lm} \mathbf{F}_{Hqp} + \tilde{e}_{qp}^{lm} \mathbf{F}_{Eqp} + \tilde{f}_{qp}^{lm} \mathbf{F}_{Lqp}) , \tag{A.8}$$

where use has been made of Eq. (A.4) and the second equality follows from the expansion of any vector field in terms of the vector spherical wavefunctions. Taking the scalar product of Eq. (A.8) with $\bar{\mathbf{F}}_{Hl'm'}$ given by

$$\bar{\mathbf{F}}_{Hl'm'} = \frac{f_{l'}}{\psi_{l'}} \left(\sqrt{2} \alpha_{l'}^{-m'} Y_{l'm'-1}^* \hat{\mathbf{e}}_+^* + \sqrt{2} \alpha_{l'}^{m'} Y_{l'm'+1}^* \hat{\mathbf{e}}_-^* + m' Y_{l'm'}^* \hat{\mathbf{e}}_0^* \right) \tag{A.9}$$

leads to

$$\sum_{qp} \bar{\mathbf{F}}_{Hl'm'} \cdot (\tilde{g}_{qp}^{lm} \mathbf{F}_{Hqp} + \tilde{e}_{qp}^{lm} \mathbf{F}_{Eqp} + \tilde{f}_{qp}^{lm} \mathbf{F}_{Lqp})$$

$$= \frac{f_{l'} f_l}{\psi_{l'} \psi_l} \left[2\alpha_{l'}^{-m'} \alpha_l^{-m}(\epsilon_r' + \epsilon_\kappa') Y_{l'm'-1}^* Y_{lm-1} \right.$$

$$\left. + 2\alpha_{l'}^{m'} \alpha_l^m(\epsilon_r' - \epsilon_\kappa') Y_{l'm'+1}^* Y_{lm+1} + m'm Y_{l'm'}^* Y_{lm} \right] . \tag{A.10}$$

Integrating both sides of Eq. (A.10) over the solid angle and taking into account the orthogonality relations (A.2) we obtain

$$\tilde{g}_{l'm'}^{lm} = \frac{(l^2 + l - m^2)\epsilon_r' + m\epsilon_\kappa' + m^2}{l(l+1)} \delta_{ll'} \delta_{mm'} . \tag{A.11}$$

Similarly, taking the scalar product of Eq. (A.8) with $\bar{\mathbf{F}}_{El'm'}$ and $\bar{\mathbf{F}}_{Ll'm'}$, and integrating over the solid angle results in two linear equations, which can be solved to give

$$\tilde{e}_{l'm'}^{lm} = \sqrt{\frac{(l-1)(l-m)(l+m)}{(l+1)(2l-1)(2l+1)}} \frac{m\bar{\epsilon}_r' - (l+1)\epsilon_\kappa'}{l} \delta_{l-1,l'} \delta_{mm'}$$

$$+ \sqrt{\frac{(l+2)(l-m+1)(l+m+1)}{l(2l+1)(2l+3)}} \frac{m\bar{\epsilon}_r' + l\epsilon_\kappa'}{l+1} \delta_{l+1,l'} \delta_{mm'} , \tag{A.12}$$

$$\tilde{f}_{l'm'}^{lm} = \sqrt{\frac{(l-m)(l+m)}{l(l+1)(2l-1)(2l+1)}}\left[m\bar{\epsilon}_r' - (l+1)\epsilon_\kappa'\right]\delta_{l-1,l'}\delta_{mm'}$$

$$-\sqrt{\frac{(l-m+1)(l+m+1)}{l(l+1)(2l+1)(2l+3)}}\left[m\bar{\epsilon}_r' + l\epsilon_\kappa'\right]\delta_{l+1,l'}\delta_{mm'}, \qquad (A.13)$$

where $\bar{\epsilon}_r' = \epsilon_r' - 1$. In the same manner, by taking the product of dyad $\epsilon_z \overset{\leftrightarrow}{\epsilon}_g^{-1}$ and vector $\mathbf{F}_{Elm}$ given by Eq. (A.6) and expanding the resulting vector $\epsilon_z \overset{\leftrightarrow}{\epsilon}_g^{-1} \mathbf{F}_{Elm}$ in terms of the vector spherical wavefunctions with expansion coefficients $\bar{g}_{qp}^{lm}$, $\bar{e}_{qp}^{lm}$, $\bar{f}_{qp}^{lm}$ leads to an equation analogous to Eq. (A.8). Taking the scalar product of this equation with $\bar{\mathbf{F}}_{Hl'm'}$, $\bar{\mathbf{F}}_{El'm'}$ and $\bar{\mathbf{F}}_{Ll'm'}$, and integrating over the solid angle gives rise to three linear equations, which can be solved to give

$$\bar{g}_{l'm'}^{lm} = \sqrt{\frac{(l+1)(l-m)(l+m)}{(l-1)(2l-1)(2l+1)}}\frac{m\bar{\epsilon}_r' + (l-1)\epsilon_\kappa'}{l}\delta_{l-1,l'}\delta_{mm'}$$

$$+\sqrt{\frac{l(l-m+1)(l+m+1)}{(l+2)(2l+1)(2l+3)}}\frac{m\bar{\epsilon}_r' - (l+2)\epsilon_\kappa'}{l+1}\delta_{l+1,l'}\delta_{mm'}, \qquad (A.14)$$

$$\bar{e}_{l'm'}^{lm} = \delta_{ll'}\delta_{mm'}$$

$$+\frac{[(2l^2+2l+3)m^2 + (2l^2+2l-3)l(l+1)]\bar{\epsilon}_r' + (4l^2+4l-3)m\epsilon_\kappa'}{l(l+1)(2l-1)(2l+3)}\delta_{ll'}\delta_{mm'}$$

$$-\sqrt{\frac{(l-2)(l+1)(l-m-1)(l-m)(l+m-1)(l+m)}{(l-1)l(2l-3)(2l+1)}}\frac{\bar{\epsilon}_r'}{2l-1}\delta_{l-2,l'}\delta_{mm'}$$

$$-\sqrt{\frac{l(l+3)(l-m+1)(l-m+2)(l+m+1)(l+m+2)}{(l+1)(l+2)(2l+1)(2l+5)}}\frac{\bar{\epsilon}_r'}{2l+3}\delta_{l+2,l'}\delta_{mm'},$$

$$(A.15)$$

$$\bar{f}_{l'm'}^{lm} = \frac{(l^2+l-3m^2)\bar{\epsilon}_r' - (2l-1)(2l+3)m\epsilon_\kappa'}{\sqrt{l(l+1)(2l-1)(2l+3)}}\delta_{ll'}\delta_{mm'}$$

$$-\sqrt{\frac{(l+1)(l-m-1)(l-m)(l+m-1)(l+m)}{l(2l-3)(2l+1)}}\frac{\bar{\epsilon}_r'}{2l-1}\delta_{l-2,l'}\delta_{mm'}$$

$$+\sqrt{\frac{l(l-m+1)(l-m+2)(l+m+1)(l+m+2)}{(l+1)(2l+1)(2l+5)}}\frac{\bar{\epsilon}_r'}{2l+3}\delta_{l+2,l'}\delta_{mm'}.$$

$$(A.16)$$

References

1. F. D. M. Haldane and S. Raghu, *Phys. Rev. Lett.* **100**, 013904 (2008).
2. S. Raghu and F. D. M. Haldane, *Phys. Rev. A* **78**, 033834 (2008).
3. Z. Wang *et al.*, *Phys. Rev. Lett.* **100**, 013905 (2008).
4. Z. Wang *et al.*, *Nature* (*London*) **461**, 772 (2009).
5. T. Ochiai and M. Onoda, *Phys. Rev. B* **80**, 155103 (2009).
6. X. Ao, Z. Lin and C. T. Chan, *Phys. Rev. B* **80**, 033105 (2009).
7. H. Zhu and C. Jiang, *Opt. Exp.* **18**, 6914 (2010).
8. J. X. Fu, R. J. Liu and Z. Y. Li, *Appl. Phys. Lett.* **97**, 041112 (2010).
9. Y. Poo *et al.*, *Phys. Rev. Lett.* **106**, 093903 (2011).
10. K. Fang, Z. Yu and S. Fan, *Phys. Rev. B* **84**, 075477 (2011).
11. K. Liu, L. Shen and S. He, *Opt. Lett.* **37**, 4110 (2012).
12. A. Figotin and I. Vitebsky, *Phys. Rev. E* **63**, 066609 (2001).
13. N. Stefanou, V. Yannopapas and A. Modinos, *Comput. Phys. Commun.* **113**, 49 (1998).
14. N. Stefanou, V. Yannopapas and A. Modinos, *Comput. Phys. Commun.* **132**, 189 (2000).
15. V. Karathanos, N. Stefanou and A. Modinos, *J. Mod. Opt.* **42**, 619 (1995).
16. V. Yannopapas, A. Modinos and N. Stefanou, *Phys. Rev. B* **68**, 193205 (2003).
17. N. Stefanou and A. Modinos, *J. Phys.: Condens. Matter* **3**, 8135 (1991).
18. C. Tserkezis *et al.*, *Phys. Rev. B* **84**, 115455 (2011).
19. G. W. Ford and S. A. Werner, *Phys. Rev. B* **18**, 6752 (1978).
20. Z. Lin and S. T. Chui, *Phys. Rev. E* **69**, 056614 (2004).
21. J. L. W. Li and W. L. Ong, *IEEE Trans. Antennas Propag.* **59**, 3370 (2011).
22. J. L. W. Li, W. L. Ong and K. H. R. Zheng, *Phys. Rev. E* **85**, 036601 (2012).
23. T. Inui, Y. Tanabe and Y. Onodera, *Group Theory and its Applications in Physics* (Springer, Berlin, 1990).
24. N. W. Ashcroft and N. D. Mermin, *Solid State Physics* (Saunders, New York, 1976).
25. V. Yannopapas, *J. Phys.: Condens. Matter* **18**, 6883 (2006).
26. V. Yannopapas, *Phys. Rev. B* **83**, 113101 (2011).
27. Z. Yu *et al.*, *Phys. Rev. Lett.* **100**, 023902 (2008).
28. M. I. Mishchenko, L. D. Travis and A. A. Lacis, *Scattering, Absorption and Emission of Light by Small Particles* (Cambridge University Press, Cambridge, UK, 2002).
29. A. B. Khanikaev *et al.*, *Appl. Phys. Lett.* **95**, 011101 (2009).